Quantum Electronics **50** (4) 315–320 (2020)

EXTREME LIGHT FIELDS AND THEIR INTERACTION WITH MATTER https://doi.org/10.1070/QEL17308

Modelling of the laser amplification process with allowance for the effect of the temperature distribution in an Yb:YAG gain element on the thermophysical and lasing characteristics of the medium

V.V. Petrov, V.A. Petrov, G.V. Kuptsov, A.V. Laptev, A.V. Kirpichnikov, E.V. Pestryakov

Abstract. **A time-dependent three-dimensional model for the laser amplification process has been constructed with allowance for the effect of the temperature distribution on the thermophysical and lasing characteristics of gain media. We have performed numerical modelling of the laser amplification process in the gain elements of a two-stage subjoule-level cryogenic laser amplifier operating at a pulse repetition rate of up to 1 kHz. It has been shown that taking into account the temperature distribution is of critical importance in calculation of cryogenically cooled laser amplifiers pumped with high-power diodes. We have found optimal diode pump parameters at which the maximum achievable pulse energy at the amplifier output can reach 300 and 570 mJ at pulse repetition rates of 1000 and 500 Hz, respectively.**

Keywords: *diode pumping, high pulse repetition rate, cryogenic temperatures, laser amplifier, heat equation.*

1. Introduction

Advances in modern laser systems combining high average and peak powers have given impetus to a variety of research studies dealing with proton and ion acceleration [1], in particular for medical applications [2], and the generation of ultrashort pulses in the near-ultraviolet and X-ray regions [3] and ensured the advent of high-energy pump sources for parametric amplifiers [4]. For many applications, key parameters include not only the repetition rate, duration, spatial shape and phase profile of pulses, but also the pulse energy. The generation and amplification of high-energy pulses with a fast pulse repetition rate (PRR) and high efficiency can be ensured by Yb^{3+}-doped lasing media. The nanosecond pulse energies reached to date at PRRs of 0.5 and 1 kHz in systems based on Yb:YAG gain elements are 1 J and 120 mJ, respectively [5, 6].

An important feature of such systems is that their gain elements are under a considerable thermal load because they are pumped by high-average-power diode lasers, which leads to significant heating of the region being pumped and, as a consequence, causes the degradation of the lasing performance of the medium and phase distortions in output amplifier stages [7]. Since both the physical and lasing properties of Yb:YAG elements depend significantly on temperature, the gain coefficient of high-power laser systems is an intricate function of pump parameters. To optimise pump parameters, one should solve a system of equations that includes balance equations, the transfer equation and the heat equation to take into account the influence of thermal effects on the laser amplification process.

Studies of how the temperature of gain elements influences the gain coefficient of laser amplifiers were reported in the literature for both fibre amplifiers [8, 9] and bulk elements [10–12]. However, in most studies the three-dimensional (3D) temperature distribution, temporal temperature evolution, the dynamics of the gain coefficient, its relation to heating, the temperature dependence of lasing and thermophysical parameters or experimentally measured parameters of systems, such as the spatial pump light profile and the dependence of the heat sink temperature on pump power, are left out of account.

To optimise pump parameters in cryogenically cooled high-PRR laser amplifiers, it is necessary to simultaneously take into account all of the above parameters and dependences. This paper presents modelling results for the laser amplification process in the gain elements of a cryogenically cooled two-stage subjoule-level laser amplifier operating at a PRR of up to 1 kHz.

2. Experimental setup

Researchers at the Institute of Laser Physics, Siberian Branch, Russian Academy of Sciences, develop principles and methods of producing components of a few-cycle high-intensity light source with carrier–envelope phase (CEP) stabilisation and a high PRR. Figure 1 shows a block diagram of the source.

The source includes a system generating CEP-stabilised pulses [13], which are injected into a parametric amplifier, and a scalable joule-level solid-state laser system operating at a high PRR [14], which is used to pump the parametric amplifier. The scalable joule-level laser system comprises a master oscillator, stretcher, regenerative amplifier, two diode-pum-

V.V. Petrov Institute of Laser Physics, Siberian Branch, Russian Academy of Sciences, prosp. Akad. Lavrent'eva 15B, 630090 Novosibirsk, Russia; Novosibirsk State University, ul. Pirogova 2, 630090 Novosibirsk, Russia; Novosibirsk State Technical University, prosp. Karla Marksa 20, 630073 Novosibirsk, Russia; e-mail: vpetv@laser.nsc.ru;
V.A. Petrov, G.V. Kuptsov Institute of Laser Physics, Siberian Branch, Russian Academy of Sciences, prosp. Akad. Lavrent'eva 15B, 630090 Novosibirsk, Russia; Novosibirsk State Technical University, prosp. Karla Marksa 20, 630073 Novosibirsk, Russia; e-mail: petrov.nstu@gmail.com;
A.V. Laptev, A.V. Kirpichnikov, E.V. Pestryakov Institute of Laser Physics, Siberian Branch, Russian Academy of Sciences, prosp. Akad. Lavrent'eva 15B, 630090 Novosibirsk, Russia

Received 26 February 2020
Kvantovaya Elektronika **50** (4) 315–320 (2020)
Translated by O.M. Tsarev

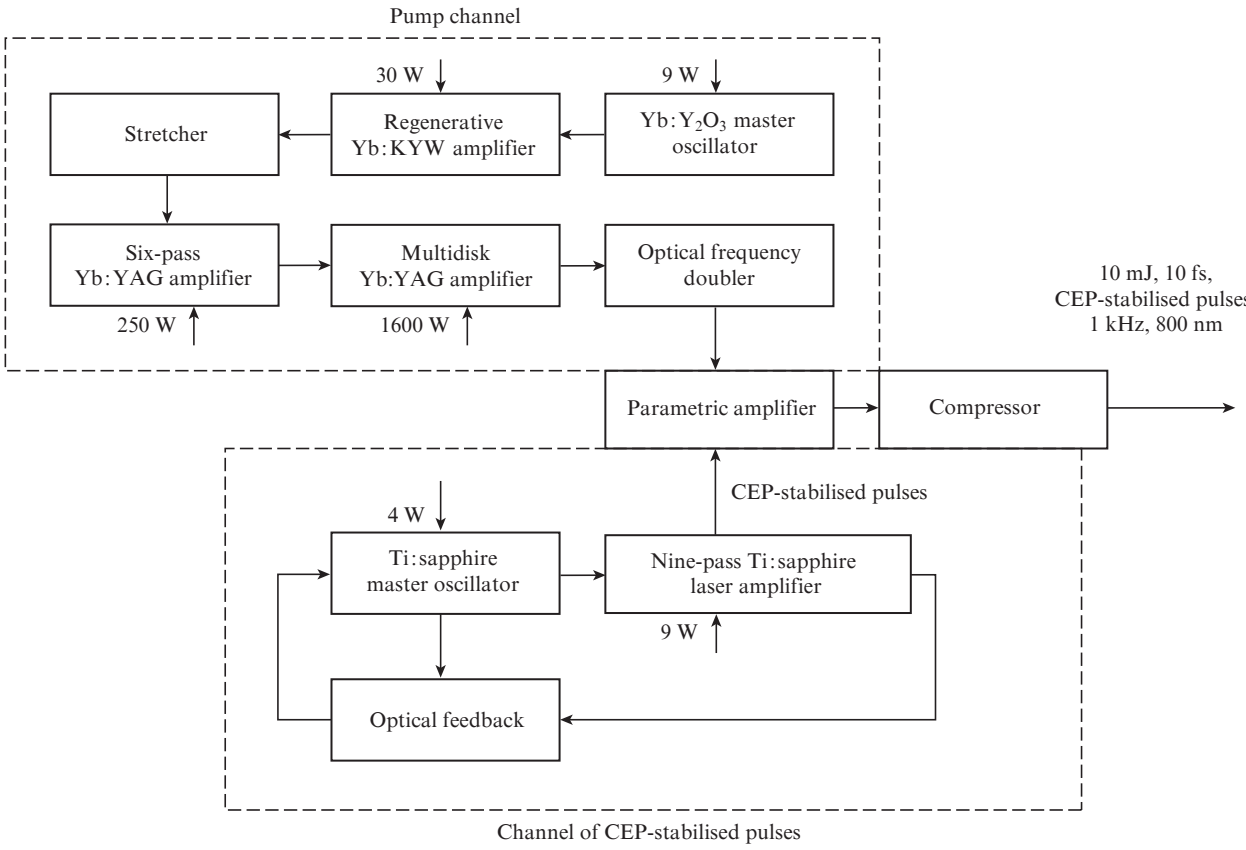

Figure 1. Block diagram of the few-cycle high-intensity light source with carrier–envelope phase stabilisation.

ped (six-pass and multidisk) laser amplifiers and an optical frequency doubler. The key component of the system is a cryogenically cooled two-stage laser amplifier pumped with a high-power diode.

The gain elements of the cryogenic amplifier are diffusion-bonded YAG–Yb:YAG crystals (10 at% Yb^{3+}), which are attached pairwise to cryogenically cooled crystal holders on the opposite sides. The crystals have the form of a disk 25 mm in diameter, in which the doped portion is 3.75 mm thick and the undoped portion is 2 mm thick. We use a total of eight gain elements, which form two amplifier stages, each consisting of four elements. Figure 2 shows a schematic of the multipass multidisk amplifier.

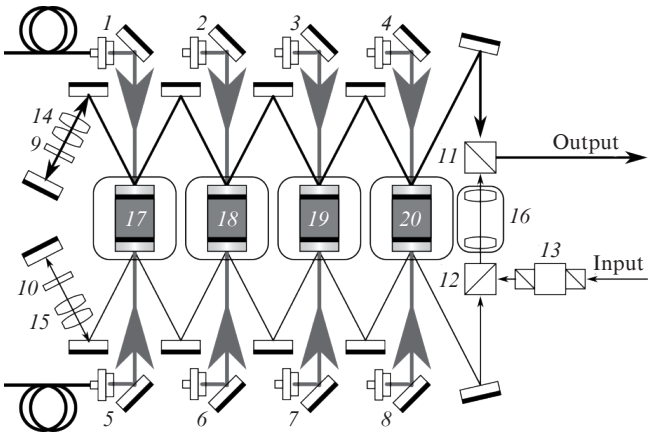

Figure 2. Schematic of the multipass multidisk amplifier: (*1–8*) fibre-pigtailed pump laser diodes; (*9*, *10*) quarter-wave plates; (*11*, *12*) polarising cubes; (*13*) Faraday isolator; (*14*, *15*) matching lens systems; (*16*) telescope in a vacuum chamber; (*17–20*) vacuum chambers with a cooling system and gain elements. The flat mirrors in the schematic are not numbered.

Propagating in the amplifier, injected pulses make a double round trip first through one and then through the other amplifier stage. The injected pulse energy at the amplifier input is 10 mJ. In the amplifier, we use eight pump laser diodes operating in continuous and quasi-continuous modes, each with a maximum power of up to 200 W and a centre wavelength of 936 nm. The gain elements of the laser amplification unit are cooled with the use of Stirling-type closed loop cryogenic cooling systems. Such coolers allow the temperature stability of gain elements to be improved, but one of their features is that the heat sink temperature is a nonlinear function of the power being dissipated [14].

3. Numerical model for laser amplification

As shown earlier [15], the temperature difference between the cooled face of a disk element in a multidisk amplifier and the face being pumped can reach ~150 K. In the temperature range 80–300 K, the absorption cross section of Yb:YAG elements varies by a factor of ~10 at the injection wavelength (1030 nm) and by a factor of ~2 at the pump wavelength; their thermal conductivity varies by a factor of 5–10 [16], depending on the doping level; and their heat capacity varies by a factor of ~5 [17]. The changes in the parameters of Yb:YAG elements by several times in going from cryogenic

to room temperatures are responsible for the nonlinear dependence of the gain coefficient on pump and cooling system parameters.

To optimise pump parameters, we constructed a time-dependent 3D numerical model that included balance equations, the transfer equation and the heat equation [16, 18]:

$$n = n(x, y, z, t), \quad T = T(x, y, z, t),$$

$$\rho(T)C(T)\frac{\partial T}{\partial t} = \nabla(\lambda(T)\nabla T) + Q,$$

$$\begin{cases} \dfrac{\partial I_\mathrm{p}}{\partial z} = -\alpha_\mathrm{a}(T) I_\mathrm{p}, \\ \dfrac{\partial n}{\partial t} = \dfrac{I_\mathrm{p}}{h\nu_\mathrm{p}}\alpha_\mathrm{a}(T) - n/\tau_\mathrm{L}, \end{cases}$$

$$\begin{cases} \dfrac{\partial I_\mathrm{L}}{\partial t} + c\dfrac{\partial I_\mathrm{L}}{\partial z} = cI_\mathrm{L}\alpha_\mathrm{L}(T) - n/\tau_\mathrm{L}, \\ \dfrac{\partial n}{\partial t} = -\dfrac{I_\mathrm{L}\alpha_\mathrm{L}(T)}{h\nu_\mathrm{p}} - n/\tau_\mathrm{L}, \end{cases}$$

$$\alpha_\mathrm{a}(T) = \sigma_\mathrm{a}(T)[(n_\mathrm{i} - n)f_{01}(T) - nf_{12}(T)],$$

$$\alpha_\mathrm{L}(T) = \sigma_\mathrm{L}(T)[nf_{11}(T) - (n_\mathrm{i} - n)f_{03}(T)],$$

$$Q(x, y, z, t) = -\eta\frac{\partial I_\mathrm{p}(x, y, z, t)}{\partial z},$$

$$f_{ji}(T) = \exp\left(-\frac{\Delta E_{ji}}{kT}\right)\left[\sum_{i=1}^{3}\exp\left(-\frac{\Delta E_{ji}}{kT}\right)\right]^{-1},$$

where n_i (cm^{-3}) is the dopant concentration; n (cm^{-3}) is the population density in the working level; T (K) is the gain element temperature; f_{ji} is the population density in the energy level E_{ji}; λ ($\mathrm{W\,cm^{-1}\,K^{-1}}$), ρ ($\mathrm{kg\,cm^{-3}}$) and C ($\mathrm{J\,K^{-1}\,kg^{-1}}$) are the thermal conductivity, density and specific heat of the medium; α_a (cm^{-1}) and σ_a (cm^2) are the absorption coefficient and absorption cross section at the pump wavelength; α_L (cm^{-1}) and σ_L (cm^2) are the absorption coefficient and absorption cross section at the wavelength of the light being amplified; η is the fraction of the absorbed pump energy converted to heat; c ($\mathrm{cm\,s}^{-1}$) is the speed of light; I_L ($\mathrm{W\,cm}^{-2}$) is the intensity of the light being amplified; I_p ($\mathrm{W\,cm}^{-2}$) is the pump intensity; τ_L (s) is the luminescence lifetime of the laser transition; and k ($\mathrm{J\,K}^{-1}$) is the Boltzmann constant. The pump beam is directed along the z axis.

The model takes into account the effect of temperature on the thermophysical and lasing parameters of the gain element [16, 17]. Calculations are performed with the use of experimentally measured spatial and temporal distribution profiles of pump light and the light being amplified and experimentally determined parameters of the closed loop cryogenic cooling system [14]. The numerical model and boundary conditions used in this work were described previously [19].

In such a model, calculations are performed in two steps. In the first step, we find the temperature field and laser level populations in the gain elements. To this end, the system of balance equations is solved jointly with the heat equation, which allows the temperature dependence of the absorption cross section of the Yb ion at the pump wavelength (936 nm) to be taken into account together with the temperature dependences of the laser level populations. The time-dependent 3D heat equation includes calculation of the temperature distributions in the gain element and components of the cryogenic cooling system. Taking into account the dynamic variation of the absorption cross section at the pump wavelength with the temperature distribution leads to a decrease in the calculated temperature gradient in the medium and a more uniform variation in the temperature distribution both along and across the pump direction.

In the second step of modelling, the transfer equation and the balance equation for the laser transition are solved jointly, with allowance for the spatiotemporal energy distribution of the pulse being amplified.

Using the proposed model, we performed numerical modelling of the laser amplification process in a gain element of a multidisk amplifier and compared the results with previously reported experimental data [14] (Fig. 3).

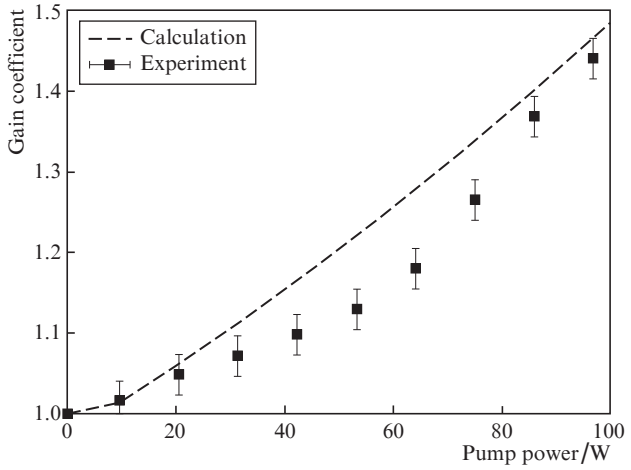

Figure 3. Comparison of the calculated gain coefficient in the multidisk amplifier with experimental data.

The discrepancy between the experimental data and modelling results can be accounted for by the facts that the amplified spontaneous emission was left out of account and that the thermophysical and lasing parameters of the particular gain element differed from data in the literature. For laser amplification in the gain element at room temperature, the model agrees well with the experimental data.

4. Discussion

To optimise the cryogenic multidisk amplifier, we modelled the laser amplification process at different spatial and temporal pump parameters. The following pump pulse parameters were used in all calculations: peak power of 200 W, third-order hyper-Gaussian spatial intensity profile, rectangular temporal profile. The pulses being amplified had a Gaussian spatial profile and a Gaussian temporal profile with a width of 1 ns (full width at half maximum). The gain coefficient was calculated as the output to input pulse energy ratio. The pump beam and the beam of the light being amplified had identical $1/e^2$ radii. The instant when the pulse being amplified arrived at the gain element coincided with the end of the pump pulse.

Figure 4 shows the gain coefficient as a function of pump beam radius for a pulse of 10 mJ energy after a double pass

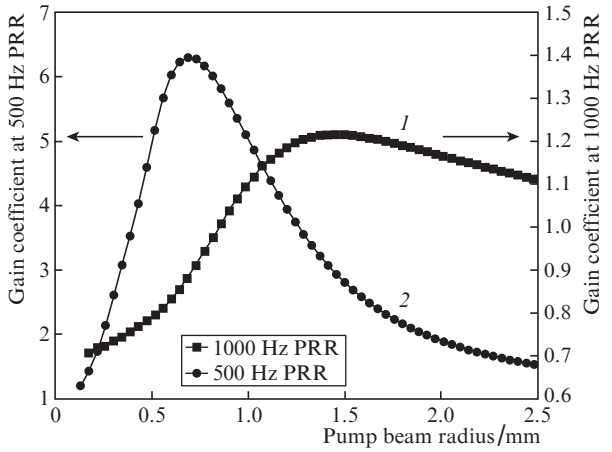

Figure 4. Gain coefficient as a function of $1/e^2$ pump beam radius at a pulse period-to-pulse duration ratio of (*1*) 2 and (*2*) 4.

through one gain element. It follows from these data that, at a given pump pulse duration, the optimal pump beam radius depends on PRR and needs to be adjusted and that the maximum achievable gain coefficient (at the optimal radius) increases by more than five times with decreasing PRR. At the same time, calculation indicates that, at a given pulse duty cycle, the gain coefficient changes by less than a factor of 2. The reason for this is that raising the average pump power leads to heating of the gain element in the region being pumped, degrading the lasing performance of the medium, and that reducing the diameters of the beam being amplified and the pump beam gives rise to a saturation effect. Because of this, there is an optimal pump pulse duration for each PRR at a given peak pump power.

Figure 5a shows the calculated optimal pump pulse duration as a function of PRR. Taking into account the above results, we modelled the gain coefficient as a function of optimal pump pulse duration at PRRs of 500 and 1000 Hz and a pump beam radius of 0.7 mm (Fig. 5b).

The shape of the curve representing the optimal pump pulse duration as a function of PRR is determined by parameters of the cooling system and the thermophysical and lasing properties of the medium. At the optimal pump pulse duration, the optimal radii of the interacting beams are almost independent of PRR, which is due to the particular relationship between the thermophysical and lasing characteristics of the gain medium. Figure 6 shows the gain coefficient as a function of pump beam radius with and without allowance for the temperature field. It is seen that heating of the medium limits the maximum achievable gain coefficient and accounts for the existence of an optimal pump beam radius.

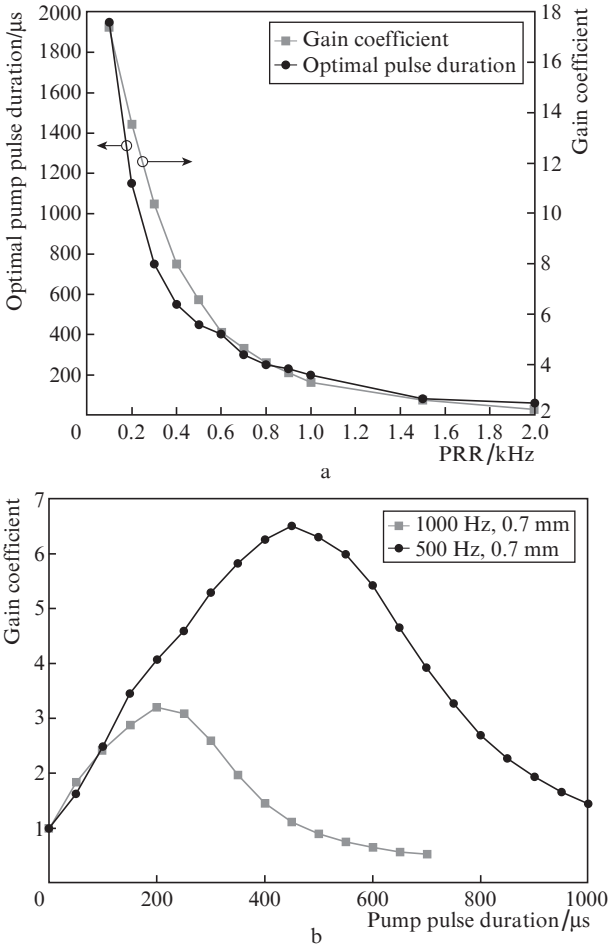

Figure 5. (a) Maximum achievable gain coefficient and optimal pump pulse duration as functions of PRR; (b) gain coefficient as a function of pump pulse duration at a constant pump beam radius.

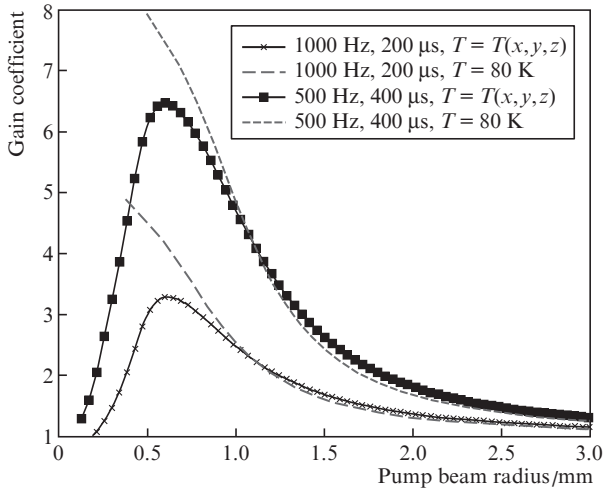

Figure 6. Gain coefficient as a function of $1/e^2$ pump beam radius at PRRs of 500 and 1000 Hz. The solid lines represent the results obtained with allowance for the temperature distribution. The dashed lines represent the calculation results obtained when the gain element temperature was taken to be constant throughout the gain element.

Taking into account the data obtained for amplification in one gain element, we calculated the gain coefficient for the first amplification stage of the multidisk amplifier using the following parameters: beam radii of 0.7 mm; pump pulse durations of 200 and 400 μs at PRRs of 1000 and 500 Hz, respectively; and input pulse energy of 10 mJ. The gain coefficients in the first stage were determined to be 13.8 and 27.3, which corresponded to injected pulse energies of 120 and 250 mJ in the second stage, with allowance for the energy loss in the optical channel at a level of ~15% per stage.

To optimise pump parameters, we performed modelling with input pulse energies of 250 and 120 mJ at PRRs of 500

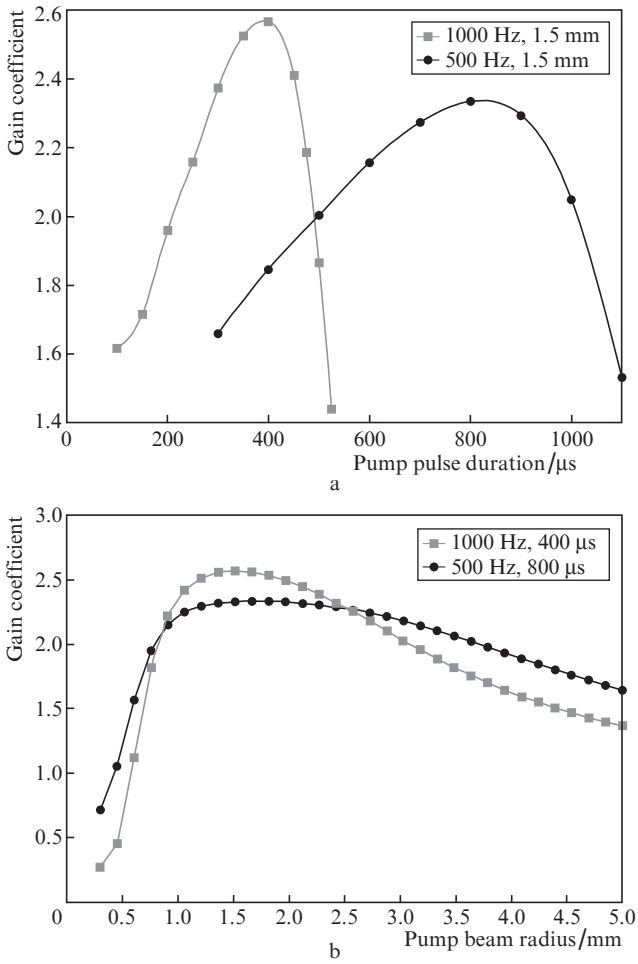

Figure 7. Gain coefficient (a) as a function of pump pulse duration at the optimal $1/e^2$ pump beam radius and (b) as a function of pump beam radius at the optimal pump pulse duration.

and 1000 Hz, respectively. The modelling results are presented in Fig. 7.

It follows from Figs 5b and 7a that the first and second amplifier stages have different optimal pump pulse durations. The reason for this is that, at a higher input injected pulse energy, a higher pump pulse energy is needed to obtain the maximum gain coefficient. Increasing the pump pulse energy through an increase in pulse duration raises the average power, leading to a larger optimal beam radius at a higher thermal load. The curves in Fig. 7b demonstrate that even a considerable increase in pump beam radius leads to only a slight decrease in gain coefficient.

The maximum achievable gain coefficients are ~2.5 and ~2.3. Therefore, the energy at the amplifier output can reach 300 and 570 mJ at PRRs of 1000 and 500 Hz, respectively.

The pump pulse energy conversion efficiency obtained in this study is difficult to achieve experimentally, but the present results make it possible to optimise laser amplifiers in terms of pump parameters. It should also be noted that the optimal radius of the pump and signal beams is limited by the breakdown threshold of dielectric coatings, which is ~2 J cm^{-2} in the case of Yb:YAG gain elements at cryogenic temperatures and a pulse duration of 1 ns [20].

5. Conclusions

We have constructed a time-dependent 3D model for the laser amplification process with allowance for the effect of the temperature distribution on the thermophysical and lasing characteristics of gain media. The model has been used for numerical modelling of the laser amplification process in the gain elements of a two-stage subjoule-level cryogenic laser amplifier operating at a PRR of up to 1 kHz. It has been shown that taking into account the temperature distribution is of critical importance in calculation of cryogenically cooled laser amplifiers pumped with high-power diodes.

Using the data obtained, we optimised diode pump parameters in the stages of a scalable two-stage subjoule-level cryogenic laser amplifier operating at a high PRR. It has been shown that optimisation allows the maximum achievable pulse energy at the amplifier output to reach 300 and 570 mJ at PRRs of 1000 and 500 Hz, respectively.

The present results make it possible to optimise amplifier parameters at cryogenic temperatures so as to maximise the signal pulse power at a preset repetition rate.

Acknowledgements. This work was supported by the Presidium of the Russian Academy of Sciences (Extreme Light Fields and Their Interaction with Matter Programme, Grant No. AAAA-A18-118040290036-4) and in part by the Russian Foundation for Basic Research (RFBR) (Project No. 20-02-00529-a), RFBR and Novosibirsk oblast government (Grant No. 19-42-543007) and the RF Ministry of Science and Higher Education (Grant No. AAAA-A17-117030310296-7).

References

1. Chvykov V., in *High Power Laser Systems* (IntechOpen, 2018) p. 63.
2. Zeil K., Baumann M., Beyreuther E., Burris-Mog T., Cowan T.E., Enghardt W., Karsch L., Kraft S.D., Laschinsky L., Metzkes J., Naum-Burger D., Oppelt M., Richter C., Sauerbrey R., Schuerer M., Schramm U., Pawelke J. *Appl. Phys. B*, **110** (4), 437 (2013).
3. Popmintchev T., Chen M., Arpin P., Murnane M., Kapteyn H. *Nat. Photonics*, **4**, 822 (2010).
4. Liu J., Wang W., Wang Z., Lv Z., Zhang Z., Wei Z. *Appl. Sci.*, **5** (4), 1590 (2015).
5. Larionov M., Neuhaus J., in *Advanced Solid State Lasers, OSA Tech. Digest* (OSA, 2014) paper ATh2A.51.
6. Baumgarten C., Pedicone M., Bravo H., Wang H., Yin L., Menoni C.S., Rocca J.J., Reagan B.A. *Opt. Lett.*, **41** (14), 3339 (2016).
7. Tamer I., Keppler S., Hornung M., Korner J., Hein J., Kaluza M.C. *Laser Photonics Rev.*, **12**, 1700211 (2017).
8. Shao H., Duan K., Zhu Y., Yan H., Yang H., Zhao W. *Optik*, **124**, 4336 (2013).
9. Hansen K.R., Alkeskjold T.T., Broeng J., Laegsgaard J. *Opt. Express*, **19**, 23965 (2011).
10. Lucianetti A., Sawicka M., Slezak O., Divoky M., Pilar J., Jambunathan V., Bonora S., Antipenkov R., Mocek T. *High Power Laser Sci. Eng.*, **2**, E13 (2014).
11. Ertel K., Banerjee S., Mason P.D., Phillips P.J., Siebold M., Hernandez-Gomez C., Collier J.C. *Opt. Express*, **19** (27), 26610 (2011).
12. Vadimova O.L., Mukhin I.B., Kuznetsov I.I., Palashov O.V., Perevezentsev E.A., Khazanov E.A. *Quantum Electron.*, **43** (3), 201 (2013) [*Kvantovaya Elektron.*, **43** (3), 201 (2013)].
13. Kirpichnikov A.V., Petrov V.V., Kuptsov G.V., Laptev A.V., Petrov V.A., Pestryakov E.V., Trunov V.I. *Proc. SPIE*, **10614**, 106140U (2018).

14. Petrov V.V., Kuptsov G.V., Petrov V.A., Laptev A.V., Kirpichnikov A.V., Pestryakov E.V., *Quantum Electron.*, **48** (4), 358 (2018) [*Kvantovaya Elektron.*, **48** (4), 358 (2018)].
15. Petrov V.V., Kuptsov G.V., Nozdrina A.I., Petrov V.A., Laptev A.V., Kirpichnikov A.V., Pestryakov E.V. *Quantum Electron.*, **49** (4), 358 (2019) [*Kvantovaya Elektron.*, **49** (4), 358 (2019)].
16. Brown D.C., Tornegård S., Kolis J., McMillen C., Moore C., Sanjeewa L., Hancock C. *Appl. Sci.*, **6**, 23 (2016).
17. Aggarwal R.L., Ripin D.J., Ochoa J.R., Fan T.Y. *J. Appl. Phys.*, **98**, 103514 (2005).
18. Brown D.C., Vitali V.A. *IEEE J. Quantum Electron.*, **47** (1), 3 (2011).
19. Petrov V.A., Kuptsov G.V., Petrov V.V., Kirpichnikov A.V., Laptev A.V., Spichak M.P., Korel I.I., Pestryakov E.V. *AIP Conf. Proc.*, **2125**, 030060 (2019).
20. Wang P., Zhang W., He H. *Appl. Opt.*, **51** (36), 8687 (2012).